



# Electric Force Microscopy, Surface Potential Imaging, and Surface Electric Modification *with the Atomic Force Microscope (AFM)*

By: F.M. Serry, K. Kjoller, J. T. Thornton,  
R. J. Tench, and D. Cook

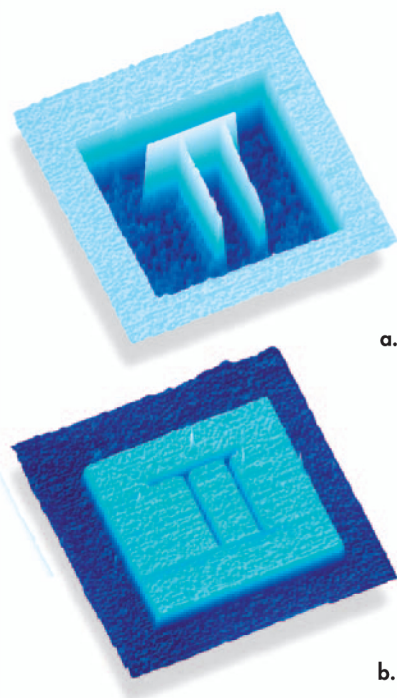


Figure 1. EFM images showing reversed tip bias from a to b of polarized ferroelectric domains in an epitaxial, single crystalline  $\text{Pb}(\text{Zr}_{0.2}\text{Ti}_{0.8})\text{O}_3$  thin film. The corresponding topography (not shown) is featureless, with  $2\text{\AA}$  RMS roughness. The polarization pattern was created using the same metal-coated AFM tip that moments later captured these images. See Figure 10 and the corresponding text.  $1.5\mu\text{m}$  scan courtesy T. Tybell, C.H. Ahn, and J.M. Triscone, University of Geneva, Switzerland.

## Introduction

Electric Force Microscopy (EFM) and Surface Potential (SP) imaging are two AFM techniques, which characterize materials for electrical properties. A conductive AFM tip interacts with the sample through long-range Coulomb forces. These interactions change the oscillation amplitude and phase of the AFM cantilever, which are detected to create EFM or SP images (see Resonance Shift, page 8). In an EFM image (Figure 1) the phase, frequency, or amplitude of the cantilever oscillation is plotted at each in-plane (X,Y) coordinate. This phase, frequency, or amplitude is related to the gradient of the electric field between the tip and the sample. In a SP image (Figure 2), variations in the surface potential on the sample are plotted. A voltage carrying AFM tip also enables electrical modification of materials on or beneath the surface, such as depicted in Figures 1 and 10.

Applications include electrical failure analysis, detecting trapped charges, quantifying contact potential difference (CPD) between metals and/or semiconductors, mapping relative strength and direction of electric polarization, testing electrical continuity, and performing electrical read/write.

## Electric Force Microscopy (EFM)

EFM is used to map the vertical (Z) and near-vertical gradient of the electric field between the tip and the sample versus the in-plane coordinates X and Y. This is done using LiftMode™ (see page 8). The field due to trapped charges—on or beneath the sample surface—is often sufficiently large to generate contrast in an EFM image. Otherwise, a field can be induced by applying a voltage between the tip and the sample. The voltage may be applied directly from the microscope's electronics under AFM software control, or from an external power supply with appropriate current-limiting elements in place. EFM is performed in one of three modes: amplitude detection, phase detection, or

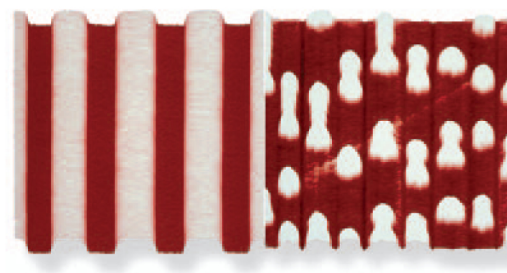


Figure 2. Topography (left) and SP image (right) of a CD-RW. The SP image locates the position of the bits. Images courtesy of Yasudo Ichikawa, Toyo Corporation, Tokyo, Japan.  $5\mu\text{m}$  scans.

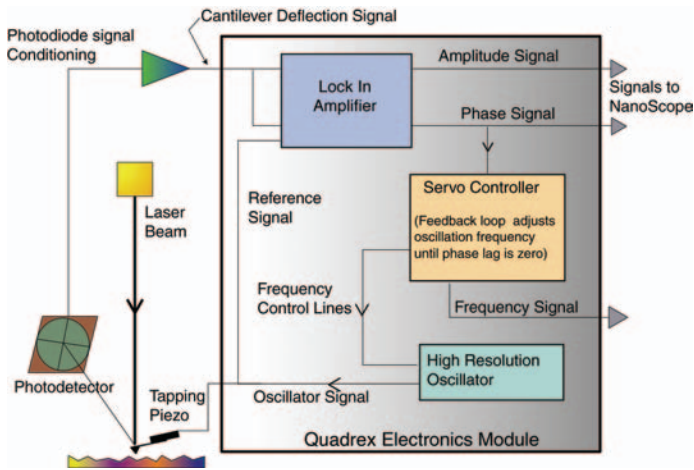


Figure 3a. Amplitude and phase detection and frequency modulation (FM) techniques for EFM.

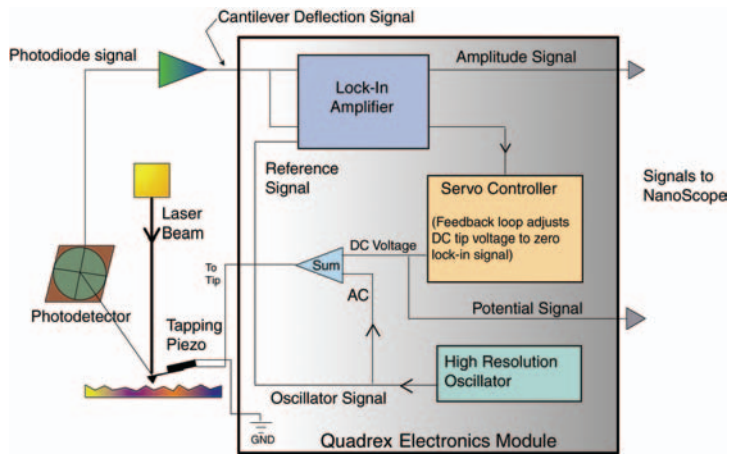


Figure 3b. Surface Potential (SP) imaging.

frequency modulation (FM). Amplitude and phase detection and FM modes are depicted in the block diagram in Figure 3a. In the amplitude and phase detection modes, there is no feedback during the LiftMode scan; i.e., the drive signal that oscillates the cantilever has constant frequency. The 3-D EFM image is generated by plotting the cantilever's phase or amplitude versus the in-plane coordinates. In the FM mode, the phase of the cantilever oscillation is measured relative to the phase of the drive signal from a high-resolution oscillator. The phase difference is used as an error signal in a feedback scheme; i.e., the frequency of the drive signal is modulated ("Frequency Control lines" in Figure 3a) to maintain the cantilever oscillation at a constant phase relative to the drive signal. The modulations of the drive signal frequency are then plotted versus the in-plane coordinates, creating the 3-D EFM image.

The preferred methods of EFM are phase detection and FM, because the cantilever's phase response is 1) faster than its amplitude response to changes in the tip-sample interactions and, 2) less susceptible to height variations on the sample surface.

## Surface Potential Imaging

Surface Potential (SP) imaging maps the electrostatic potential on the sample surface with or without a voltage applied to the sample.<sup>1</sup> SP imaging is a nulling technique. As the tip travels above the sample surface in LiftMode, the tip and the cantilever experience a force wherever the potential on the surface is different from the potential of the tip. The force is nullified by varying the voltage of the tip so that the tip is at the same potential as the region of the sample surface underneath it. The voltage applied to the tip in nullifying the force is plotted versus the in-plane coordinates, creating the surface 3-dimension potential image.

Figure 3b depicts the SP imaging technique. During the LiftMode scan, the piezoelectric element that mechanically drives the cantilever in TappingMode™ height imaging is idle. Instead, an adjustable AC electric signal at, or near, the cantilever's fundamental resonance frequency is applied directly to the tip. In the presence of a DC potential difference between the tip and the sample, the AC signal gives rise to a periodic Coulomb force which has the right frequency to drive the cantilever into resonant mechanical oscillation. The

DC voltage of the tip is then adjusted by feedback electronics until the tip and the sample are at the same potential, where the frequency of the periodic Coulomb force on the cantilever is now twice the fundamental resonance frequency.

## Examples of Applications

In the topography image (Figure 4a) the shallow pit near the center would be indistinguishable from the many similarly sized features in view. Yet, the corresponding SP image (Figure 4b) clearly singles out this pit, about 160mV higher in potential than the surrounding area. This locally high potential region was one of many on this aluminum sample. The cause of the higher potential was unknown.

SP imaging can sometimes detect material contamination and defects in manufacturing. The regularly-spaced features in the topography scan in Figure 5a are 200nm-tall tungsten islands, patterned out of a blanket tungsten film by etching. The substrate is silicon. In the SP image (Figure 5b), the randomly sized and spaced dark regions on the tungsten islands are lower in potential than the surrounding areas. Their relatively sharp boundaries

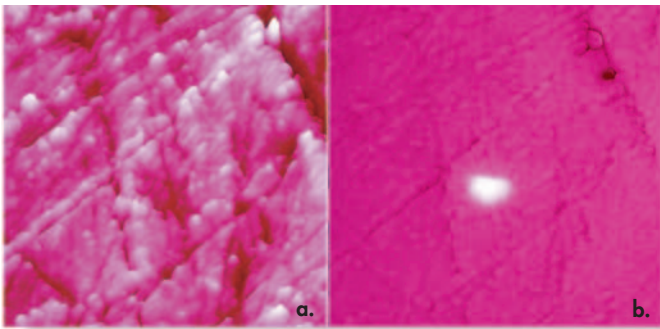


Figure 4. Topography (a) and SP images (b) of a sample of aluminum. Interpretation of the images is not always straight forward (see text). 8.8 $\mu$ m scans.

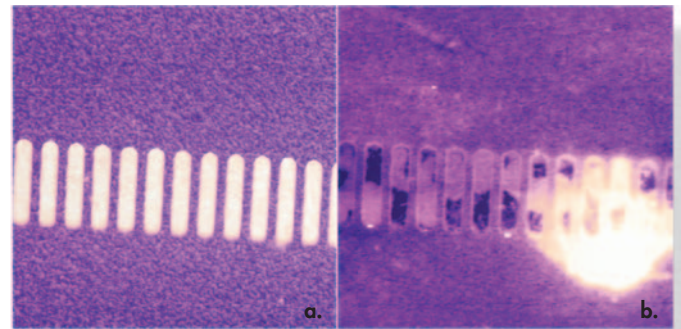
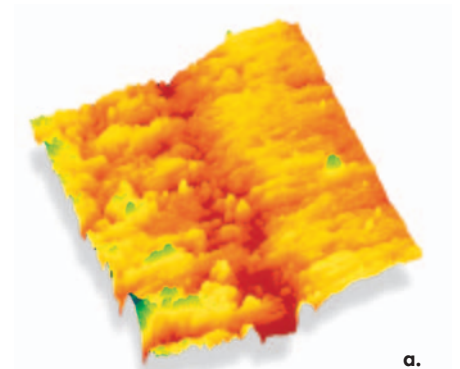


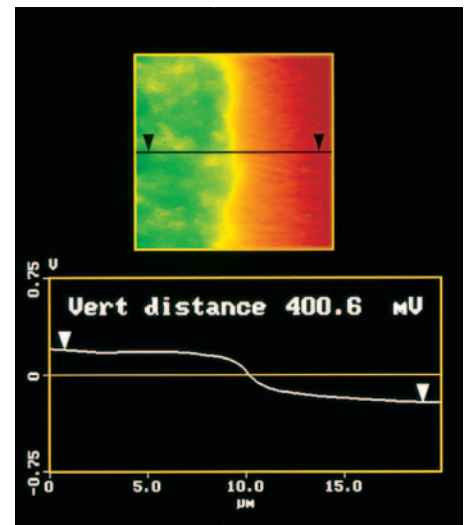
Figure 5. Topography (a) and SP images (b) of tungsten islands on silicon substrate. Darker regions correspond to lower potential in the SP image. 76 $\mu$ m scans.

suggest that the source of the contrast is right on the surface. Their random pattern suggests a likely cause for these low-potential regions: trapped charge in photoresist residue left over after the tungsten etching process. On the other hand, the bright, high-potential region on the lower right of the SP image is diffuse and largely indiscriminant of tungsten and silicon. This suggests that the source of this contrast may be beneath the surface, perhaps in the silicon substrate. Note that the topography is devoid of any features corresponding to the contrasts visible in the SP image. Images like those in Figures 5 can help in early detection of potential causes of device failure such as revealed in Figure 6, discussed next.

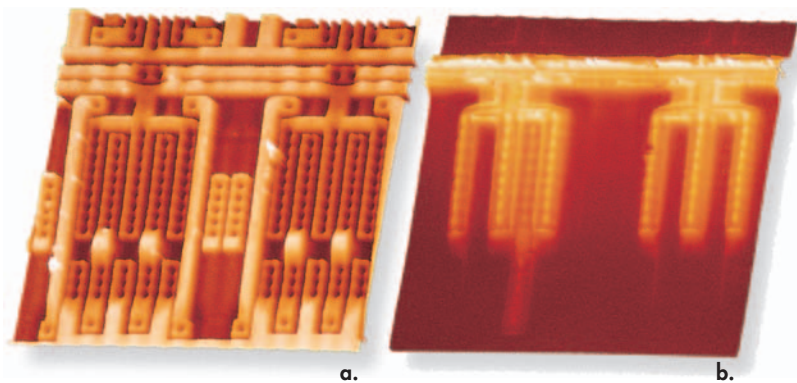
EFM is a useful failure analysis tool on the device, wafer, or chip level—even on packaged IC's. The images in Figures 6 are from a region on a packaged SRAM IC with the passivation layer still on and with voltage applied to select bus lines. All of the devices along this region had voltages applied in the three-pronged arrangement seen in the right half of the EFM image in Figure 6b — all except for the device shown on the left half of this image. The electric signal between the second and third prongs from the left shows that the transistor on the left is in saturation. The topography image in Figure 6a shows no hint of this failure. Using emission microscopy first, a defect was detected in the vicinity of



a.



b.



a.

b.

Figure 6. Topography (a) and EFM image (b) of a live packaged IC with passivation layer on. EFM image detects transistor in saturation. 80 $\mu$ m scans.

Figure 7. Topography (a) and SP image (b) (with cross-section) across the boundary between aluminum and copper. CPD measures ~400mV. Sample courtesy of P. Schmutz and G. Frankel, Ohio State University. 20 $\mu$ m scans.



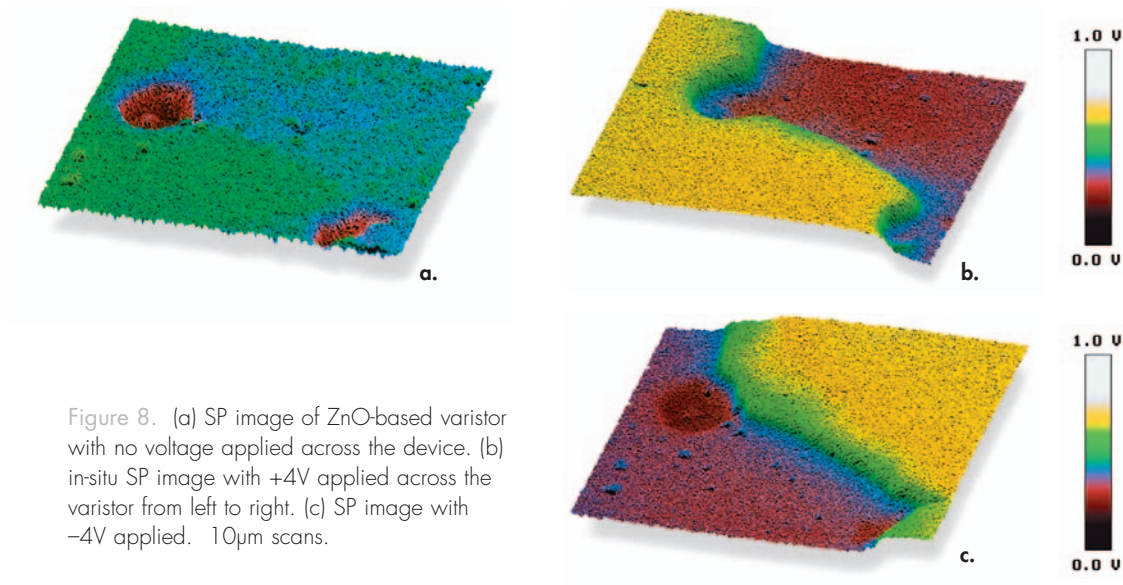


Figure 8. (a) SP image of ZnO-based varistor with no voltage applied across the device. (b) in-situ SP image with +4V applied across the varistor from left to right. (c) SP image with -4V applied. 10 $\mu$ m scans.

this transistor, but the cause and the exact location of the defect were not identifiable until the EFM image was captured. With the passivation removed, and then reactive ion etch strip-back to the gate oxide, AFM topography images of another defective transistor very close to this area revealed an ESD (electrostatic discharge)-induced rupture hole in the gate oxide of that transistor (not shown).

SP imaging can be used to detect and quantify contact potential differences (CPD) on the surface. In Figures 7 the topography (a) and the SP (b) images are shown across a boundary that separates aluminum from copper. Topography shows the copper on the right has polished differently than the aluminum on the left. The contrast in the SP image is due to the CPD across the two metals. An average cross section measurement on the SP image returns a value of about 400mV, which is close to the difference of the work functions of the two metals—but not equal to it since the imaging was performed in air, rather than vacuum.

Grain boundary potential barriers in polycrystalline materials play important roles in the electronic properties of devices such as solar cells, gas sensors, variable-temperature-coefficient resistors, and varistors (variable resistors or surge protectors). The applied-voltage dependence and spatial variation of grain boundary potential barriers can be quantified using SP imaging, as shown by Huey and Bonnell (University of Pennsylvania), who have studied the resistance across boundaries of electrically active grains *in-situ*; i.e., on varistors and similar devices in operation.

In a varistor, the electrical resistance across a grain boundary can be up to 1000 times larger than that across a grain, thus becoming the major impediment to current flow. Figure 8a shows the SP image of a region on the surface of a zinc oxide (ZnO)-based varistor device with no applied bias voltage across the device. The image depicts two low-potential islands and a faint boundary that runs from upper left to lower right. EDS (Energy Dispersive Spectroscopy) chemical data using a SEM showed the low-potential islands to be second phases rich in Ti and Bi.

The island near the top is approximately 100mV lower in potential than the region to the left of the faint boundary. The potential drop across the faint boundary itself is only about 1.5mV. The contrasts in this image are attributable to differences in work function across the boundaries. Figures 8b and c show the SP images of the same area when (b) +4 volts and, (c) -4 volts are externally applied to the varistor from left to right. Electron back scattering pattern microscopy (EBSP) confirmed that the voltage steps in these images mark the location of a grain boundary in the zinc oxide. The tall potential steps in these images reveal the resistive nature of the grain boundaries. SP images not only pinpoint the location of the grain boundary—absent in the topography image (not shown)—but also enable measurement of the potential drop across it (approximately 350mV). With knowledge of the carrier (donor) concentration in the ZnO grains and of the magnitude of the current flowing through the varistor during *in-situ* AFM imaging, measurements of these voltage steps can be used to calculate the grain boundary potential barrier.

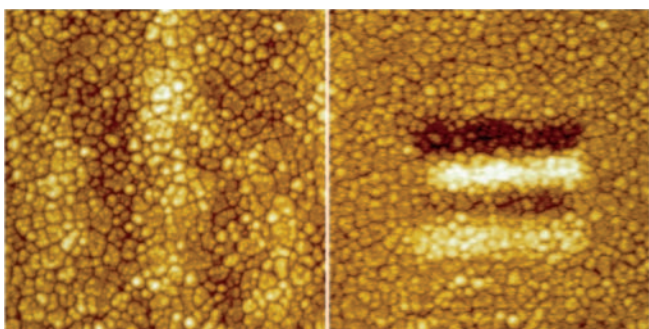


Figure 9. Topography (left) and FM-EFM (right) images of a ferroelectric film with electrical bits written onto it. The four bits were written with a metal-coated AFM tip at +3,-3,+2, and -2volts from top to bottom. The images were captured with the same tip, moments after polarizing the central region. Carrying +1V, the tip failed to polarize this ferroelectric film. 2 $\mu$ m scans.

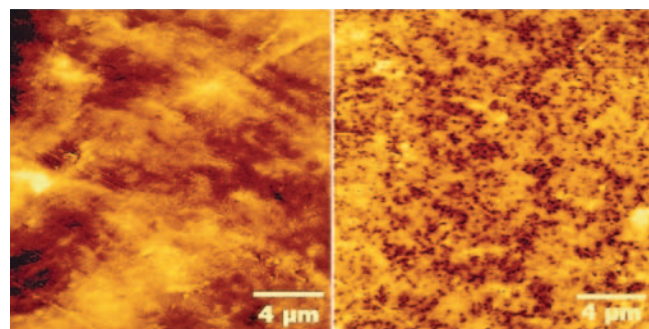


Figure 10. On the surface of a conductor-insulator composite, topography (left), EFM image (right) allows easy identification and measurement of carbon black network (dark regions) leading to calculation of fractal dimension and correlation length in corroboration with SEM-based results. 16 $\mu$ m scans.

By locally polarizing ferroelectric materials, an AFM can create what is tantamount to electrical bits. At Advanced Surface Microscopy, Don Chernoff uses TappingMode AFM with a metal-coated tip to “write” onto a ferroelectric thin film and then uses the same tip in LiftMode to “read” the polarization just induced.<sup>2</sup> Figure 9 illustrates this. The background pattern which appears in both images is due to the grain boundaries on the surface of the ferroelectric film. At the center of the EFM image, four polarized regions are identified with a metal-coated AFM tip, the same tip which was biased with a DC voltage to induce the polarization just moments earlier. With the polarity of the tip reversed from 700mV to -1500mV during imaging (i.e., during the “reading”), the contrast of the four bits was reversed (not shown). This verified that the electrical bits were indeed stored in the ferroelectric film. The size of a bit is determined in part by the sharpness of the AFM tip, and in part by the properties of the ferroelectric film and the voltage required to achieve the desired level of polarization. The typical radius of curvature at the apex

of a metal-coated TappingMode AFM tip is 25-50nm. (See also images in Figures 1a,b)

The electrical transport properties of disordered conductor-insulator composites are closely tied to the structure of their “percolation network,” which enables the movement of charge carriers through the composite. Figure 10 shows the topography (left) and the EFM image of an area on the surface of a 250 $\mu$ m-thick sample of a disordered conductor-insulator composite, with small islands of conductive carbon-black randomly dispersed within the non-conductive high-density polyethylene matrix. Some of the carbon-black islands are isolated from one another, while others are connected in a continuous network—an “infinite cluster”—so that they create a conductive path through the thickness of the composite. The EFM image was captured with a 3V potential difference between the tip and the sample. The dark areas in the EFM image are parts of the carbon-black infinite cluster. The lighter colored areas depict the material not in the infinite cluster; i.e., the non-conductive polymer and the isolated islands of carbon-black. The EFM

image was quantified using grain analysis, enabling calculation of the fractal dimension (2.6 $\pm$ 0.1) and estimation of the correlation length (~3 $\mu$ m) for the percolation network. These numerical results corroborated findings from electron microscopy image analysis on other similar carbon black composites.<sup>3</sup> It is known that such composites do not conduct electricity (i.e., the infinite cluster does not form), if the volume fraction of the conducting material is less than a certain “percolation threshold.” For this composite, the percolation threshold is reported in other literature to be 0.170 +/- 0.001.<sup>4</sup> EFM images of a sample of this composite with carbon black volume fraction of 0.168 (slightly less than the percolation threshold) did not show any contrast even when the tip voltage was increased. On the other hand, a sample with carbon black volume fraction of 0.179 (slightly larger than the percolation threshold) revealed contrast, but with a correlation length larger than that of the 0.1978-volume-fraction sample, which is shown in the figures here. This work was done by Ravi Viswanathan and Michael Heaney at Raychem Corporation, Menlo Park, California.<sup>5</sup>

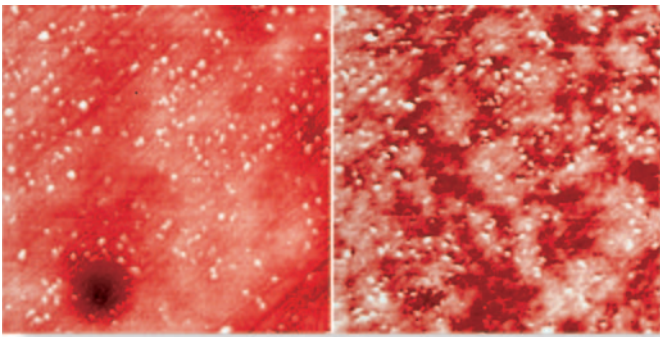


Figure 11. Topography (left) and phase detection EFM (right) images of the surface of a thick-film resistor (TFR). EFM image depicts the conductive RuO<sub>2</sub> network (dark) exposed at the surface. 56µm scans.

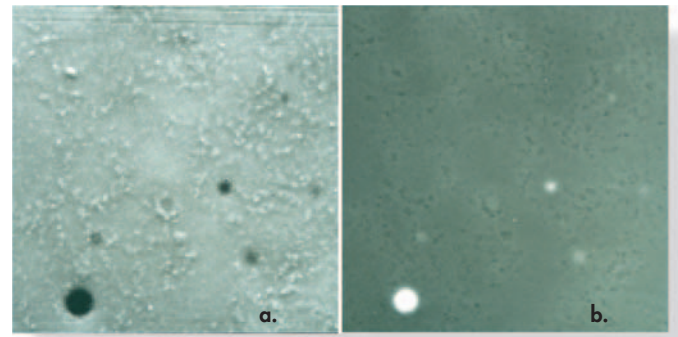


Figure 12. Secondary electron (SE) SEM image (a) and sample current (SC) image (b) identify the same areas distinguished as conductive (green) in the EFM image in Figure 11. Images are ~56µm square.

EFM has also proven useful in similar studies on thick-film resistors (TFR). TFR are composites used in hybrid thick-film microelectronics and sensors; for example, as heating elements in printing heads of equipment such as facsimiles and printers. As an electric current is forced through it, a TFR heats up and makes a permanent mark on a heat-sensitive paper. The uniformity of heat generation in the TFR and the transfer of the heat to the paper (and thus the quality of print marks produced on paper) depend on a number of parameters, including the sub-micron structure of the percolation network in TFR. RuO<sub>2</sub>-glass composites are commonly used as TFR heating elements in printing heads, and have been studied by Andreas Alessandrini and

Giovanni Valdrè at the Physics department at the University of Bologna, Italy. In Figure 11 the topography (left) and EFM (phase detection) images are shown for such a composite with a 20V DC potential applied to the sample relative to the grounded tip. Small protrusions speckle the topography image and are also convoluted into the EFM image. The contrast between lighter and darker red areas in the EFM image depends on the applied voltage; the green areas are part of the percolation network. These same areas are also depicted in a secondary electron (SE) SEM image (Figure 12a) as well as in a sample current (SC) image (Figure 12b). Secondary electron and EDS analysis revealed that these green areas were indeed RuO<sub>2</sub> crystals.

Figure 13 shows TappingMode AFM topography and EFM images of a cross-section of a nanowire bundle embedded in a matrix of the dielectric Al<sub>2</sub>O<sub>3</sub> (alumina). The cross-section was polished and some of the dielectric was etched; the nanowires are protruding out of the matrix slightly and showing up as lighter colored regions (taller) in topography (left). Nanowire composites such as these may be used in making high-density electrical multi-feedthroughs and photosensing arrays. An external voltage (~7V relative to the grounded tip) was applied to the other end of the bundle, and the electric field gradient was monitored in LiftMode using amplitude detection at this end of the bundle. One of the nanowires (marked by **x** in the topography image) is not

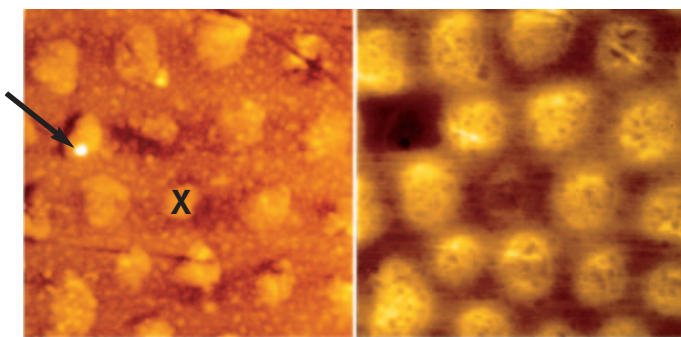


Figure 13. Topography (left) and EFM (right) images of cross-section of a nanowire bundle embedded in an alumina matrix. EFM image locates a broken nanowire (marked by "X") and some trapped charge (darker, upper left). 1.7µm scans.

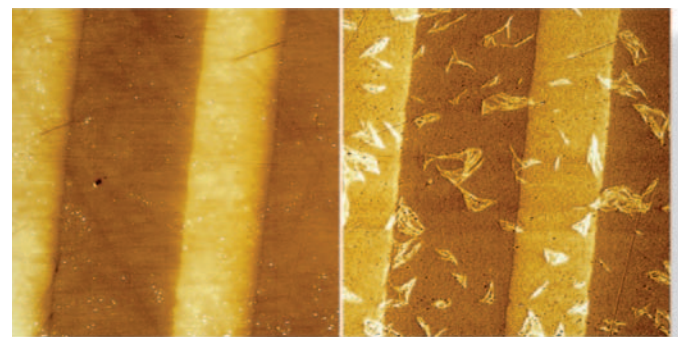


Figure 14. Topography (left) and Surface Potential image (right) of alternating TiO<sub>2</sub> and SiO<sub>2</sub> regions. SP image shows the CPD and debris on the surface. 40µm scans.



showing contrast in the EFM image, indicating discontinuity in the wire. The EFM image also detects a region of high electric field gradient on the upper left (dark region). The source of this high field gradient is unknown, but possibly trapped charge in a particle (indicated by an arrow), which is resting on the surface as revealed in the topography image. This work was done by Tito Huber and his colleagues at Polytechnic University, New York; Howard University, Washington DC; Naval Surface Warfare Center, Silver Spring, MD; and Veeco Instruments.<sup>6</sup>

Figure 14 shows the topography and the SP image captured on the cross section of a multi-layer of alternating  $\text{SiO}_2$  and  $\text{TiO}_2$ , which was mechanically polished (using colloidal alumina particles) at a shallow angle to expose the different layers. The two materials polished differently, giving rise to topographic contrast. The SP image shows the contact potential difference (CPD) between the  $\text{TiO}_2$  (lighter color) and the  $\text{SiO}_2$ . In addition, the SP image depicts small regions of locally-higher potential dispersed over the entire image. These are debris (likely  $\text{SiO}_2$ ) left over from the polishing process.

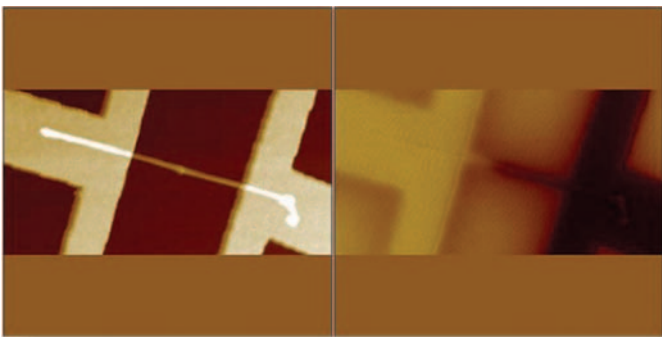


Figure 15. Topography (left) and Surface Potential (right) images of an IP-based nanowire between two metal contacts with biased applied between them.  $2\mu\text{m} \times 1\mu\text{m}$  scans. Sample courtesy of Philips Corp., The Netherlands.

---

## Summary

Electric Force Microscopy (EFM) and Surface Potential (SP) imaging are non-destructive AFM techniques for detecting electric field gradients and surface potential variations on insulating, conducting and semiconducting materials. Requiring little or no sample preparation, characterization is done in air on test structures and materials in research – on chip- or wafer-level devices, and even on completed, powered ICs. Applications range from monitoring fabrication processes, to failure analysis, to quantifying electrical properties of materials. In addition to imaging, a conductive AFM tip with a controlled voltage can be used to modify electrical properties of materials locally, e.g., polarization of ferroelectric films.

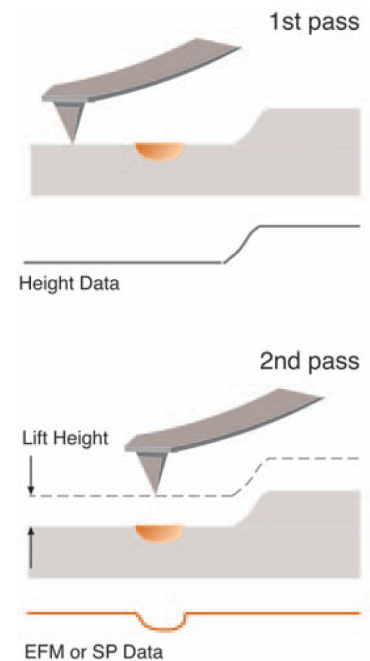


## References

1. Surface Potential imaging is sometimes referred to as Scanning Kelvin Probe Microscopy (SKPM)
2. Advanced Surface Microscopy, Indianapolis, IN, USA.
3. F. Ehrburger-Dolle and M. Tence, Carbon, Volume 28, p. 448, 1990.
4. M. B. Heaney, Physical Review B, Volume 52, 12477, 1995.
5. R. Viswanathan and M. B. Heaney, "Direct Imaging of the Percolation Network in a Three-Dimensional Disordered Conductor-Insulator Composite," Physical Review Letters, Volume 75, Number 24, pp. 4433-4436, 11 December 1995.
6. C. A. Huber, T.E. Huber, M. Sadoqi, L. A. Lubin, S. Manalis, and C. B. Prater, "Nanowire Array Composites," Science, Volume 263, pp. 800-802, 11 February 1994.

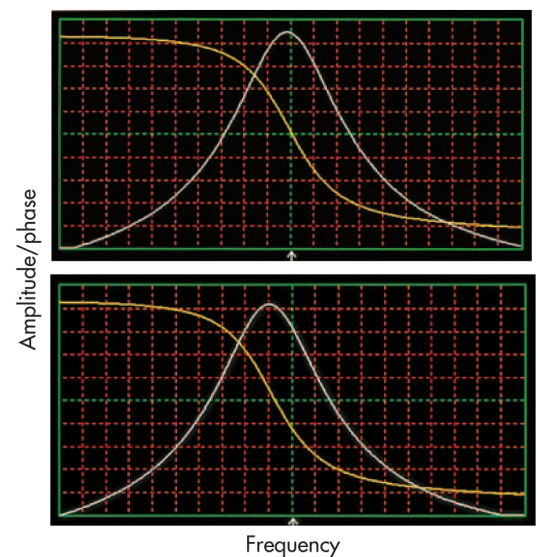
## LiftMode

If not compensated for, height variations on the sample surface can diminish the fidelity of EFM and SP images. A patented two-pass AFM technique, addresses this issue. For each scan line, the height (topography) data is recorded in TappingMode during the first pass (see Veeco Instruments Application Note on TappingMode Imaging and Technology). Then, in the second pass, the tip lifts above the surface to an adjustable “lift height,” typically 5-50nm, and scans the same line while following the height profile recorded in the first pass. The EFM or SP data is generated during the second pass — in LiftMode. In the diagrams, the orange-colored region in the sample symbolizes the source of contrast in the EFM or SP image.



## Resonance Shift

A conductive AFM tip can interact with the sample through long-range Coulomb forces: Amplitude (white) and phase (yellow) resonance response of a metal-coated AFM cantilever/tip above a sample of aluminum, held at 0V (top) and 10V (bottom) relative to the grounded tip. The tip is never in contact with the sample. In the presence of the electric field (bottom plot), the tip experiences an attractive force toward the sample. Effectively, the stiffness (spring constant) and thus the resonance frequency of the cantilever is reduced; the entire resonance curve shifts down along the frequency axis (horizontal). Changes in the cantilever’s amplitude and phase are used to characterize electrical properties on, or just beneath, the surface of the sample.



### WORLDWIDE CUSTOMER SUPPORT FROM THE INDUSTRY LEADER

Bruker Corporation is a leading provider of high-performance scientific instruments and solutions for molecular and materials research, as well as for industrial and applied analysis. For more information, visit [www.bruker.com](http://www.bruker.com), email [productinfo@bruker-nano.com](mailto:productinfo@bruker-nano.com), or call +1.805.967.1400/800.873.9750.